Journal of Nuclear Medicine, published on January 8, 2021 as doi:10.2967/jnumed.120.252429

Simulation of low dose protocols for myocardial perfusion ^{82}Rubidium imaging

Martin Lyngby Lassen[1,2], Yuka Otaki[1], Paul Kavanagh[1], Robert J.H. Miller[1,3], Daniel S. Berman[1], and Piotr J. Slomka[1]

[1]Department of Imaging and Medicine, Cedars-Sinai Medical Center, Los Angeles, CA, USA

[2]Department of Clinical Physiology, Nuclear Medicine and PET and Cluster for Molecular Imaging, Rigshospitalet, University of Copenhagen, Copenhagen, Denmark

[3]Libin cardiovascular institute, University of Calgary, Calgary, Canada

First author is a postdoctoral fellow in training:
Martin Lyngby Lassen, PhD
Artificial Intelligence in Medicine Program
Cedars-Sinai Medical Center
8700 Beverly Blvd Ste A047N
Los Angeles, California 90048 USA
Email: martin.lyngby.lassen@regionh.dk

Corresponding author: Piotr Slomka, Artificial Intelligence in Medicine, Cedars-Sinai Medical Center, 8700 Beverly Boulevard, Metro 203, Los Angeles, CA 90048, USA. Tel.: 310-423-4348, Fax: 310-423-0173.
Email: piotr.slomka@cshs.org

Word count: 5360

Short title: Low dose ^{82}Rb PET MPI

Abstract

Purpose

Quantification of myocardial perfusion and myocardial blood flow using Rubidium-82 (^{82}Rb) positron emission tomography (PET) is increasingly utilized for assessment of coronary artery disease (CAD). Current guidelines suggest injections of 1100-1500MBq. Reducing the injected dose avoids PET system saturation in first-pass flow images and reduces radiation exposure, but the impact on myocardial perfusion quantification on static perfusion images is not fully understood. In this study, we aimed to evaluate the feasibility of performing myocardial perfusion scans using either a half-dose (HfD) or quarter dose (QD) protocol using reconstructions from acquired full-dose (FD) scans.

Methods

This study comprised 171 patients who underwent rest/stress ^{82}Rb PET with a 3D 4-ring PET/CT scanner using a FD protocol and invasive coronary angiography within 6 months of the PET emission scan. HfD and QD reconstructions were obtained by using the prescribed percentage of events from the FD listmode files. Total perfusion deficit for rest (rTPD), stress (sTPD) and ischemia (ITPD = sTPD-

rTPD) were quantified. Diagnostic accuracy for obstructive CAD, defined as stenosis ≥70% in any of the three major coronary arteries, was compared with area under the receiver operating characteristic curve (AUC).

Results

Patients with a median BMI of 28.0 (Inter quartile range = 23.9-31.7) were injected with doses of 1,165±189 MBq ^{82}Rb. For sTPD, FD and HfD protocols had similar AUC (FD = 0.807, HfD = 0.802, p=0.108), whereas QD had reduced AUC (0.786, p=0.037). There was no difference in AUC obtained for ITPD among the three protocols (AUC: FD=0.831, HfD = 0.835, QD = 0.831, all p≥0.805).

Conclusion

Half-dose imaging does not affect the quantitative diagnostic accuracy of ^{82}Rb PET on 3D PET/CT systems and could be used clinically.

Keywords: myocardial perfusion imaging, positron emission tomography, rubidium, low dose

Abbreviations:

AUC: area under the receiver operating characteristic curve

CAD: Coronary artery disease

FD: full-dose

HfD: half-dose

QD: quarter-dose

ICA: invasive coronary angiography

MBF: myocardial blood flow

MPI: myocardial perfusion imaging

NECR: noise equivalent count rate

PET: positron emission tomography

^{82}Rb: Rubidium-82

SDS: summed difference score

SRS: summed rest score

SSS: summed stress score

TPD: total perfusion deficit

INTRODUCTION

Myocardial perfusion imaging (MPI) is one of the most commonly performed diagnostic tests in cardiology, with several tracers existing for positron emission tomography (PET) (*1*). Of these, 82-Rubidium (^{82}Rb) is one of the most widely used tracers as it permits quantification of myocardial blood flow (MBF) and MPI in centers without access to cyclotrons (*2*–*4*). Current guidelines from both North America (*1*,*4*) and Europe (*5*) are still based on the older 2D PET technology and suggest injections of 1,100-1,500MBq ^{82}Rb for cardiac PET. In our recent study (*6*), we found that halving the dose reduced the risk of PET system saturation (0% reported cases) in comparison to a full-dose protocol (20% reported cases) for the myocardial blood flow protocols. However, it is not fully understood how ^{82}Rb injected dose reduction would affect the quantitation of relative myocardial perfusion from static images, which remains the key clinical assessment (*4*,*5*).

To this end, this study evaluated if the use of a half-dose (HfD) and a quarter dose (QD) protocol affects the diagnostic accuracy of static myocardial perfusion of ^{82}Rb using reconstructions obtained from the full dose data.

METHODS

Study Population

In total, 171 patients without prior history of coronary artery disease (CAD) were included retrospectively in this study. History of CAD was defined as previous myocardial infarction or revascularization (*7*). All patients underwent a routine ^{82}Rb rest/stress PET imaging protocol using either adenosine (99 patients, 58%) or regadenoson (72 patients, 42%) pharmacologic stress. This study only included patients who had invasive coronary angiography (ICA) within 6 months (mean 14 days, range 0-170) according to clinical indications (*8*). The institutional review board approved this retrospective study and all subjects signed a written informed consent.

Imaging Protocol and Dose Reduction

All patients underwent rest/stress imaging protocols in a Siemens Biograph 64 TruePoint with True V using targeted doses of 925-1,500MBq for both rest and stress MPI depending on the age of the ^{82}Rb generator (*8*). The patients were instructed to abstain from all caffeine for 24h before the tests, fast for at least 6 hours, and not take antianginal drugs on the morning of the test. A low dose computed tomography (CT) attenuation correction scan was acquired for both PET studies

(100kV, pitch 1.5, 11mAs). Pharmacological stressing of the patients was acquired using intravenous infusion of adenosine (140mg/kg/min, duration 6 minutes) or bolus injection of regadenoson (0.4mg). Stress MPI scans were initiated 3 minutes after initiation of adenosine injection or 10-20 seconds after injection of regadenoson to ensure optimal coronary vasodilation, with images acquired for six minutes.

Dose Reduction

HfD and QD reconstructions were obtained from the FD scans by selecting subsets of the recorded events from the FD listmode files with replacement of the removed counts using randomized sampling with bootstrapped selection of the data (*9*). For the HfD and QD scans, the count rates of the true events were reduced linearly, reflecting the dose reduction (HfD: 1:2, QD: 1:4), whereas the random events were downsampled using a square reduction of the count rates to compensate for the changes in noise equivalent count rate (NECR) (**Figure 1**) (*10*). While the NECR curves are system-specific, the NECR curves follow the same patterns until PET system saturation is achieved. Utilizing the reduced listmode files, 3D sinograms were created for both the HfD and QD scans.

Image Reconstructions

Static PET images were reconstructed using 4 minutes of data, starting at the 2nd minute following injection of ^{82}Rb to ensure blood pool clearance of ^{82}Rb (*8*). All datasets were reconstructed in batch mode using a vendor-provided reconstruction toolbox (JS Recon, Siemens Knoxville, USA). The reconstructions employed an attenuation weighted ordered-subset expectation maximization reconstruction algorithm (iterative reconstruction) employing 4 iterations and 4 subsets, followed by a Butterworth filtration (cutoff frequency of 5Hz, order of 12). The images were reconstructed using a 256x256x109 matrix, resulting in a spatial resolution of 4.07x4.07x2.03mm. An additional image series of data reconstructed using 3 iterations and 24 subsets, followed by an 8mm Gaussian filtration was also evaluated. All PET images were reconstructed using automatic registration of the CT attenuation correction maps when deemed necessary by the technologists (*8*).

Image Processing and Quantitative Perfusion Assessment

All images were processed automatically in a batch-mode format using QPET software (Cedars-Sinai Medical Center, Los Angeles, California) (*11*). The left ventricle was delineated automatically (*12*) and corrected manually by a nuclear

cardiology expert when deemed necessary (*8*). The accuracy of the automatic segmentation of the left ventricular wall was based on visual assessments, including evaluations of the blood pool activity and the uptake patterns observed for the blood pool and left ventricular wall. All assessments were performed by an experienced nuclear medicine specialist. Rest and stress total perfusion deficit (rTPD and sTPD, respectively) were reported for all patients (*13*). Ischemic total perfusion deficit (ITPD) was calculated as the difference between the sTPD and rTPD. The overall analyses including all 171 patients, as well as two subgroups (BMI<30 (N=109), and BMI≥30 (N=62)), were evaluated to test for differences in the quantitative assessment of obese and normal-to-overweight patients.

Image Quality

To assess the overall image quality of the data, contrast-to-noise ratio (CNR), and blood pool noise measured as the coefficient of variation were calculated for all images (*14*). The overall noise in images was calculated as the coefficient of variation obtained in the left ventricular blood pool (**Figure 2**):

$$\text{Blood pool noise} = \frac{stdev(blood\ pool)}{mean(\ blood\ pool)}$$

In the equation, the stdev represents the standard deviation obtained for the blood pool.

CNR was calculated as the difference in the average uptake in the myocardium and blood pool, divided by the noise in the blood pool (calculated as the standard deviation):

$$CNR = \frac{mean(ventricular_{VOI}) - mean\ (blood\ pool)}{stdev\ (blood\ pool)}$$

In the equation, $ventricular_{VOI}$ represents the segmentation of the left ventricle.

All quantitative image quality parameters were derived fully automatically in batch mode. The blood pool noise and CNR were calculated from automatic segmentations of the left ventricle and blood pool, which were shrunk by 60% to limit the spillover effects between blood and tissue uptake (**Figure 2**). The blood pool ROIs are generated by contracting the endocardial walls with respect to the mid myocardial wall.

Invasive Coronary Angiography

Patients had ICA within 14±27 days of MPI during the study period ranging from January 2008 to September 2012. Stenosis severity was evaluated by two experienced interventional cardiologists. Stenosis of ≥70% of the left artery

descending, left circumflex or right coronary arteries, or ≥50% for the left main arteries were considered as the presence of obstructive CAD.

Statistical Analysis

Continuous variables are presented as mean and standard deviations. Categorical variables are presented as absolute numbers with percentages. Statistical analyses were performed with Analyse-it software (version 5.40.2, Analyse-it Software Ltd). Receiver operating characteristic curves analyses were compared using the DeLong and DeLong method (*15*), using the area under the curve (AUC) as the primary end-point for this study. The correlation between the FD and HfD/QD images were reported as Bland-Altman plots and repeatability coefficients (RC). Comparisons of CNR and blood pool noise were performed using Kruskal-Wallis tests. Differences in requirements for manual adjustments for automatic segmentation of the left ventricle were calculated using Chi^2 statistics in R. P-values <0.05 were considered significant.

RESULTS

Injected Doses and Patient Characteristics

The patients were injected with 1,165±189 MBq ^{82}Rb for the MPI scans (FD dose scans), while reduced dose reconstructions were equivalent to 581±100 MBq (HfD) and 290±50 MBq (QD), respectively. The corresponding body weight corrected doses were equivalent to 15.0±3.8 MBq/kg, 7.5±1.9 MBq/kg, and 3.8±1.0 MBq/kg for the FD, HfD, and QD protocols, respectively. Patient characteristics are shown in **Table 1**.

Automatic Segmentation of Left Ventricle

Automatic segmenting of the left ventricle was successful without the need for manual adjustment of contours on either rest and stress scans in 90.1% (154/171), 86.0% (147/171) and 83.0% (142/171) of the cases for the FD, HfD and QD reconstructions, respectively (**Table 2**). There were no significant differences in the need for manual adjustments (**Table 2**).

Quantification

sTPD and ITPD were quantified successfully for all 171 patients for FD, HfD, and QD protocols. One-hundred eleven (65%) of the 171 patients had automatic

registration of the PET emission data and CT attenuation correction maps performed (*8*).

Stress Perfusion Analysis

In total, 47 patients had single-vessel CAD, 26 patients had two-vessel CAD and 22 patients had three-vessel CAD (**Table 1**). Diagnostic accuracy for obstructive CAD was calculated for sTPD quantification for all three reconstructions (FD, HfD, and QD). Similar AUC was reported for the FD and HfD reconstructions (AUC: FD = 0.807, HfD = 0.802, p=0.108), while the QD reconstructions had reduced AUC compared to FD scans (0.786, p=0.037) (**Figure 3A**). No differences were reported in the AUC analyses for FD, HfD and QD protocols in patients with BMI<30 and BMI≥30, likewise, no differences in the AUC analyses were observed in the quantitative accuracy for the two groups (**Supplementary Figure 1**). Results obtained for the second image series is shown in **Supplementary figure 2**. Bland-Altman plots revealed that sTPD assessments were comparable to the FD and HfD reconstructions (p=0.08), while a bias of 3% (p=0.01) was observed between the FD versus QD assessments (**Supplementary Figure 3**), results for the two subgroups are shown in **Supplementary figures 4 and 5**. RC of 5% and 7% were reported for

the FD when compared to the HfD and QD, respectively (**Supplementary Figure 3**). No dependency on the bias and body weight corrected doses were observed (**Supplementary Figure 3**). Similarly, no BMI dependency on the bias was observed for the two subgroups (**Supplementary figures 4 and 5**).

Ischemic Perfusion Analysis

No differences in diagnostic accuracy were observed for ITPD obtained using the FD, HfD, and QD protocols with AUCs of 0.831, 0.835, and 0.831 (all $p \geq 0.805$), respectively (**Figure 3B**). Comparable ITPD assessments were obtained for all three reconstruction protocols, with corresponding high reproducibility for the FD, HfD, and QD protocols, respectively (RC: FD versus HfD: 3.6%, FD versus QD: 5.0%). No differences in the AUC were observed for the two patient groups (BMI<30 and BMI≥30) for the three reconstruction protocols (**Supplementary Figure 1C-D**).

Image Quality

CNR was comparable across the three reconstruction protocols (all $p>0.19$, Kruskal-Wallis test) (**Figure 4A**) (**Table 3**). Analyses on the blood pool revealed significantly increased noise for the dose-reduced reconstructions (both $p<0.0001$) (**Figure 4B**). Results obtained for the second image series is shown in

supplementary figure 6. A case example to illustrate image quality across reconstructions is shown in **Figure 5**.

DISCUSSION

This study evaluated the impact of reducing the injected dose of ^{82}Rb MPI scans using the current guidelines for static quantitative perfusion assessments in 3D PET systems (*1*,*4*). The main finding was that MPI using a HfD imaging protocol provided similar diagnostic accuracy for obstructive CAD as the FD protocol for both sTPD and ITPD. No dependency between body weight corrected doses and changes in sTPD and ITPD were observed with reduced dose reconstructions and there was no significant change in CNR. Therefore, our results suggest that radiation doses could be halved, while maintaining diagnostic accuracy for static perfusion imaging.

The main aim of our study was to evaluate the impact of reducing the dose to half and quarter of the current dose recommendations utilized for static MPI assessments when employing ^{82}Rb (*1*,*4*,*5*). Previous studies have reported significant risks of PET system saturation during first-pass dynamic studies when injecting doses of 1100-1500MBq (30-40mCi) (*6*,*16*), as suggested by both North

American and European guidelines (*1*,*4*,*5*). Recommendations to prevent PET system saturation during the first 2 minutes of the dynamic scans include: continuous dose inflow over 30 seconds (*17*–*19*), the use of weight-specific doses (*20*), and the use of fixed doses (*16*). However, the use of fixed doses is more feasible in many centers. In a previous study from our center (*6*), utilization of a half-dose protocol did not affect MBF estimates of rest studies repeated in a small group of patients. In the current study, we confirm the validity of the reduced dose ^{82}Rb PET protocols for the main clinical component of these studies –myocardial perfusion assessment.

While repetition of the tracer injection at lower doses is necessary when estimating MBF and system saturation during the first-pass bolus of ^{82}Rb (*6*), the dose reductions in this study were obtained retrospectively from the FD listmode files. Simulating dose-reductions from listmode files is permissible because PET system saturation is not possible when performing static perfusion imaging (image reconstructions starting 2 min after tracer injection) while employing current guideline-recommended injection profiles (*4*,*5*). During the static MPI reconstructions, the local tracer uptake in the myocardium measured by the PET system will follow the system-specific detection patterns revealed in the NECR plots.

These curves are mainly used to describe the NECR, yet they also provide insight into how the detection of true and random events change when the injected activity is reduced (**Figure 1**). Common for all PET systems is that the dose-dependent changes in the measured true coincidences can be approximated by a linear relationship until PET system saturation is achieved, while the random events develop almost by an squared increase in counts when doubling the dose (*10*). By correcting the count rates (true and random) accordingly, it is possible to achieve true simulations of the half-dose and quarter dose scans.

Similar diagnostic accuracy was observed for the FD and HfD protocols, both for the grouped analyses and each of the subgroups of patients (BMI<30, BMI≥30) with low variability in results, suggesting that a 50% reduction of the injected activity is permissible without affecting the clinical utility.

No dose-weight dependent differences were reported for the rTPD and sTPD assessment in reduced dose reconstructions (**Supplementary Figure 3**). These findings are of importance as ^{82}Rb generators have continuous decay throughout their lifecycle, which affects both the injected dose and time spent on dose injection. Furthermore, no BMI dependent differences were reported for the sTPD and ITPD

assessments (**supplementary figures 1, 4 and 5**). The reliability of the rTPD, sTPD and ITPD assessments with lower dose shown in this study indicate that the changes in the dose-profile during delivery for FD scans would not affect quantitative perfusion assessment. Additionally, high accuracies of the automatic segmentation were reported for all reconstruction protocols, with manual adjustments required in 10-15% of the cases consistent with previous reports (*21*). The reduced doses led to increased noise levels, assessed as the coefficient of variation obtained in the blood pool which should be homogenous (**Figures 4 and 5**). While there was increased noise in the images, the CNR was preserved for the HfD and QD protocols. This suggests that the reduction in the dose would not significantly impact the diagnostic quality of the static perfusion images when reducing the injected dose by 50%. This finding is in concordance with the findings reported in a previous study from our center evaluating the feasibility of using a HfD protocol in the assessment of MBF (*6*). Using the HfD protocol for the MBF imaging is beneficial for two reasons, first, the use of a HfD protocol significantly reduces the risks of PET system saturation during the first 2 minutes of the acquisition. In our previous study, it was reported that datasets with PET system saturation (assessments of presence of

speckle-noise, input function shape, and identification of alternations in the sinograms) had false-positive high blood flows when compared to the blood-flows observed for studies using a HfD protocol, and to scans without observable PET system saturation (*6*). Secondly, the use of a HfD protocol also introduces a radiation dose for the patient, which is in concordance with the as low as responsible achievable principle. Furthermore, no dependency between injected doses, nor BMI and the quantitative assessments were observed in this current study. The findings of this and our previous study (*6*) suggest that the use of a HfD protocol is permissible in the assessment of MBF and perfusion defects.

This study has several limitations. First, we relied on simulations rather than acquiring separate FD, HfD, and QD scans. However, acquiring both FD, HfD, and QD datasets using the respective injection protocols would not be possible, given the increased radiation exposure this would result in for patients. Another limitation of this study was that the impact of the HfD protocol was not tested on ECG-gated data. Further evaluation of the suitability of the low dose protocols for the reporting of the ejection fraction with ^{82}Rb imaging with 8 or 16 bin protocols will need to be evaluated. Furthermore, this study was performed on a PET/CT system from a

specific vendor. Finally, the contrast and CNR measurements obtained in the study might be affected by differences in the rTPD and sTPD assessments within the segmented myocardium as the areas with perfusion defects were not removed from the analyses.

CONCLUSIONS

We report that reducing the ^{82}Rb dose by half does not affect the diagnostic accuracy of quantitative myocardial perfusion analysis for PET data obtained on 3D PET/CT systems. Based on these findings, we suggest that dose reductions of 50% could be applied in perfusion ^{82}Rb PET studies.

Acknowledgments

This study was supported in part by Siemens Medical Systems.

Financial disclosure:

PS, DB, and PK all receive royalties from Cedars-Sinai. No other relevant financial disclosures exist to this manuscript.

Key points:

Question: How do reductions of 50% and 75% of injected doses of ^{82}Rb affect quantitative assessments of myocardial perfusion?

Pertinent findings:

In total, 171 patients underwent ICA within 14±27 days of PET MPI for suspected CAD. Dose-reductions of 50% and 75% were simulated by removing counts from the acquired PET list data. The diagnostic accuracy of a half-dose reconstruction for obstructive CAD was similar to the full-dose reconstruction, while the quarter dose reconstruction was associated with reduced diagnostic accuracy.

Implications for patient care:

Reducing the injected radiotracer doses by 50% reduces patient radiation exposure and does not impact the diagnostic accuracy of quantitative assessment of perfusion.

References

1. Murthy VL, Bateman TM, Beanlands RS, et al. Clinical quantification of myocardial blood flow using PET: joint position paper of the SNMMI Cardiovascular Council and the ASNC. *J Nucl Med*. 2018;59:273-293.
2. Lortie M, Beanlands RSB, Yoshinaga K, Klein R, DaSilva JN, DeKemp RA. Quantification of myocardial blood flow with 82Rb dynamic PET imaging. *Eur J Nucl Med Mol Imaging*. 2007;34:1765-1774.
3. Bateman TM, Dilsizian V, Beanlands RS, et al. American Society of Nuclear Cardiology and Society of Nuclear Medicine and Molecular Imaging joint position statement on the clinical indications for myocardial perfusion PET. *J Nucl Med*. 2016;57:1654-1656.
4. Dilsizian V, Bacharach SL, Beanlands RS, et al. ASNC imaging guidelines/SNMMI procedure standard for positron emission tomography (PET) nuclear cardiology procedures. *J Nucl Cardiol*. 2016;23:1187-1226.
5. Hesse B, Tägil K, Cuocolo A, et al. EANM/ESC procedural guidelines for myocardial perfusion imaging in nuclear cardiology. *Eur J Nucl Med Mol Imaging*. 2005;32:855-897.

6. Lassen ML, Manabe O, Otaki Y, et al. 3D PET/CT 82Rb PET myocardial blood flow quantification: comparison of half-dose and full-dose protocols. *Eur J Nucl Med Mol Imaging*. 2020;47:3084-3093.

7. Miller RJH, Klein E, Gransar H, et al. Prognostic significance of previous myocardial infarction and previous revascularization in patients undergoing SPECT MPI. *Int J Cardiol*. 2020;313:9-15.

8. Slomka PJ, Diaz-Zamudio M, Dey D, et al. Automatic registration of misaligned CT attenuation correction maps in Rb-82 PET/CT improves detection of angiographically significant coronary artery disease. *J Nucl Cardiol*. 2015;22:1285-1295.

9. Markiewicz PJ, Thielemans K, Schott JM, et al. Rapid processing of PET list-mode data for efficient uncertainty estimation and data analysis. *Phys Med Biol*. 2016;61:N322.

10. DiFilippo FP. Instrumentation and Principles of Imaging: PET. In: Di Carli MF, Lipton MJ. Cardiac PET and PET/CT Imaging. Springer; 2007:3-18.

11. Germano G, Kavanagh PB, Slomka PJ, Van Kriekinge SD, Pollard G, Berman DS. Quantitation in gated perfusion SPECT imaging: the Cedars-Sinai

approach. *J Nucl Cardiol*. 2007;14:433-454.

12. Otaki Y, Lassen ML, Manabe O, et al. Short-term repeatability of myocardial blood flow using 82 Rb PET/CT: The effect of arterial input function position and motion correction. *J Nucl Cardiol*. 2019:1-8.

13. Slomka PJ, Nishina H, Berman DS, et al. Automated quantification of myocardial perfusion SPECT using simplified normal limits. *J Nucl Cardiol*. 2005;12:66-77.

14. Le Meunier L, Slomka PJ, Dey D, et al. Motion frozen 18F-FDG cardiac PET. *J Nucl Cardiol*. 2011;18:259-266.

15. DeLong ER, DeLong DM, Clarke-Pearson DL. Comparing the areas under two or more correlated receiver operating characteristic curves: a nonparametric approach. *Biometrics*. 1988:837-845.

16. Tout D, Tonge CM, Muthu S, Arumugam P. Assessment of a protocol for routine simultaneous myocardial blood flow measurement and standard myocardial perfusion imaging with rubidium-82 on a high count rate positron emission tomography system. *Nucl Med Commun*. 2012;33:1202-1211.

17. Klein R, Ocneanu A, deKemp RA. Time-frame sampling for 82Rb PET flow

quantification: Towards standardization of clinical protocols. *J Nucl Cardiol*. 2017;24:1530-1534.

18. Lautamäki R, Brown TLY, Merrill J, Bengel FM. CT-based attenuation correction in 82Rb-myocardial perfusion PET-CT: Incidence of misalignment and effect on regional tracer distribution. *Eur J Nucl Med Mol Imaging*. 2008;35:305-310.

19. Lautamäki R, George RT, Kitagawa K, et al. Rubidium-82 PET-CT for quantitative assessment of myocardial blood flow: Validation in a canine model of coronary artery stenosis. *Eur J Nucl Med Mol Imaging*. 2009;36:576-586.

20. Renaud JM, Yip K, Guimond J, et al. Characterization of 3-Dimensional PET Systems for accurate quantification of myocardial blood flow. *J Nucl Med*. 2017;58:103-109.

21. Nakazato R, Berman DS, Dey D, et al. Automated quantitative Rb-82 3D PET/CT myocardial perfusion imaging: Normal limits and correlation with invasive coronary angiography. *J Nucl Cardiol*. 2012;19:265-276.

22. Jakoby BW, Bercier Y, Watson CC, Bendriem B, Townsend DW. Performance characteristics of a new LSO PET/CT scanner with extended axial field-of-view

and PSF reconstruction. *IEEE Trans Nucl Sci*. 2009;56:633-639.

Tables

Table 1. Participant characteristics.

Characteristics	
Age (years)	Median =70 (IQR = 62-77)
Sex (male)	108 (63%)
CAD Risk Factors	
BMI (kg/m^2)	Median =28.0 (IQR = 23.9-31.7)
Hypertension	130 (76%)
Diabetes mellitus	63 (37%)
Smoking	24 (14%)
Family history of CAD	25 (15%)
Invasive Coronary Angiogram Findings	
Nonsignificant CAD	70 (41%)
Single vessel CAD	47 (27%)
Double vessel CAD	26 (15%)
Triple vessel CAD	22 (13%)
LM ≥ 50%	12 (7 %)
LAD ≥ 70%	65 (38 %)

LCx ≥ 70%	46 (27 %)
RCA ≥ 70%	54 (32 %)

Continuous variables are reported by median and IQR; categorical variables are reported as n(%). CAD = Coronary artery disease, BMI = Body mass index, LM = Left Main, LAD = left anterior descending, LCx = left circumflex, RCA = right coronary artery.

Table 2. The success rate of automatic delineations of the left ventricle in QPET. Numbers given in parentheses are the number of patients. p-values were obtained using Chi^2 analyses.

	Rest	Stress	No corrections needed for both rest and stress scans
FD	90.6% (155)	91.8% (157)	90.1% (154)
HfD	89.5% (153) (p=0.856)	87.1% (149) (p=0.217)	86.0% (147) (p=0.318)
QD	88.3% (151) (p=0.597)	84.8% (145) (p=0.064)	83.0% (142) (p=0.081)

FD = full dose, HfD = half dose, QD = quarter dose

Table 3. Contrast to noise ratio and blood pool noise observed for the 171 patients presented as median [Quartile 1, Quartile 3]. P-values obtained between the FD and corresponding low-dose studies are shown in parenthesis. P-values <0.05 shown in bold.

	CNR		
	Rest	Stress	Combined
FD	11.7 [8.7, 15.8]	10.7 [8.2, 13.7]	10.9 [8.3, 14.9]
HfD	10.7 [8.3, 14.3] (p=0.30)	10.3 [8.5, 13.1] (p=0.37)	10.7 [8.4, 13.5] (p=0.23)
QD	9.7 [7.6, 12.3] (p=0.38)	9.9 [7.8, 12.9] (p=0.34)	9.7 [7.6, 12.8] (p=0.22)
	Blood pool noise		
	Rest	Stress	Combined
FD	0.10 [0.07, 0.14]	0.13 [0.10, 0.17]	0.12 [0.09, 0.15]
HfD	0.13 [0.10, 0.17] **(p<0.01)**	0.15 [0.13, 0.21] **(p<0.01)**	0.14 [0.11, 0.19] **(p<0.01)**
QD	0.14 [0.11, 0.28] **(p<0.01)**	0.17 [0.13, 0.21] **(p<0.01)**	0.15 [0.12, 0.20] **(p<0.01)**

CNR = contrast to noise ratio, FD = full dose, HfD = Half dose, QD = quarter dose

Figure legends

Fig. 1 Simulation of HfD and QD protocols. HfD and QD protocols were simulated by removing counts from the list mode data following the changes in true and random events (*22*). A depicts the count rates detected in the PET system for various activities in the tissues, obtained for the FD acquisition and the simulated HfD and QD protocols. In A, the dose reduction for the prompt events are shown; the events (E_x) were removed randomly (grayed out counts) by removing half (HfD) or 75% (QD) of the counts following the NECR curves (B). In B, the blue curve represents the random measurements detected by the system, which changes as an approximate square reduction when halving the dose. C shows the sinograms obtained for the acquired PET data, while D and E show the simulated HfD and QD sinograms used for the reconstructions. The count reductions were performed directly in the PET list data, sampling events between the 2^{nd} and 6^{th} minute. Importantly, the contrast in C-E is scaled according to the count rate obtained for the FD scan and, thus, significantly reduced. FD = full dose, HfD = half-dose, QD = quarter dose

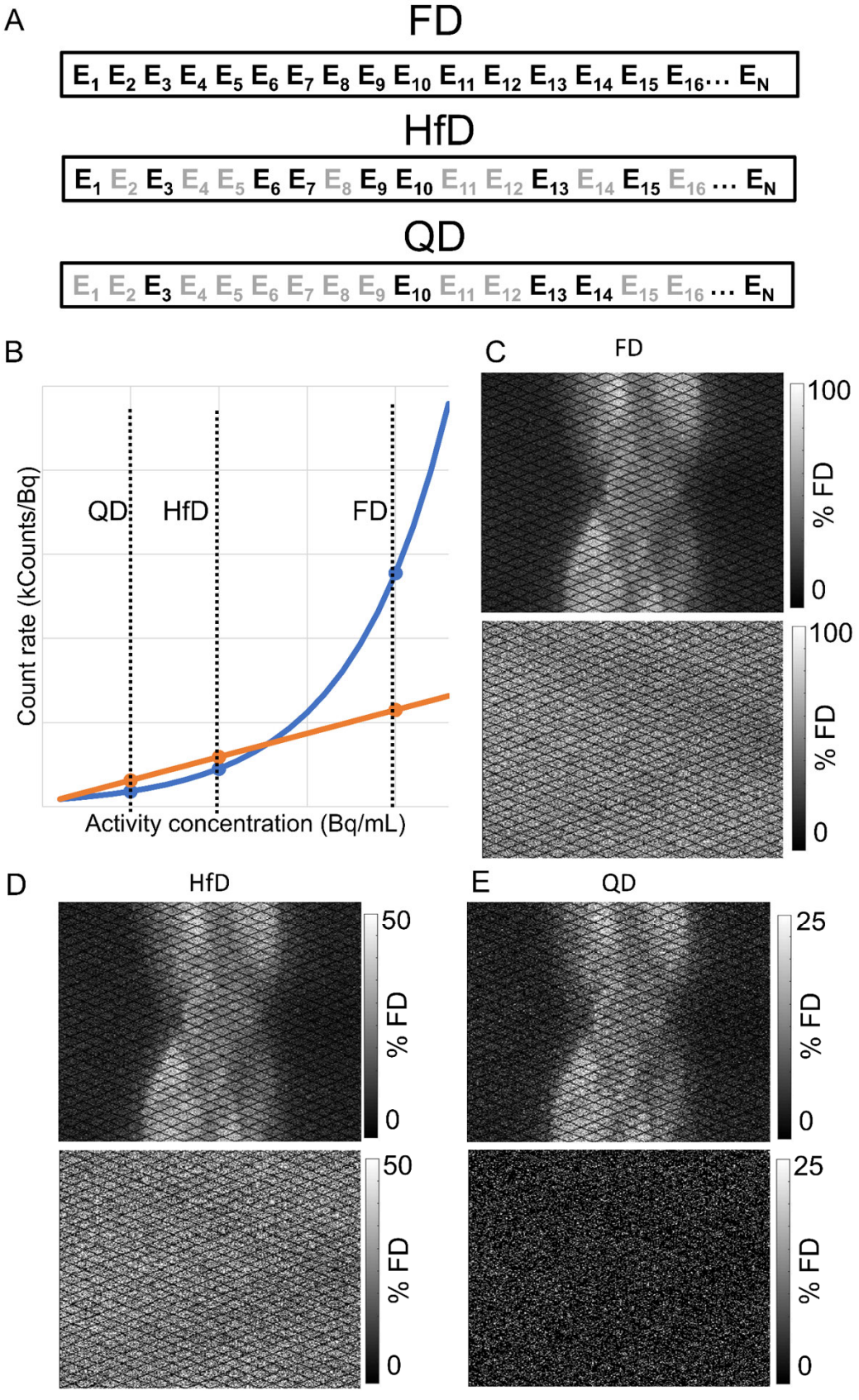
A
FD
E1 E2 E3 E4 E5 E6 E7 E8 E9 E10 E11 E12 E13 E14 E15 E16… EN
HfD
E1 E2 E3 E4 E5 E6 E7 E8 E9 E10 E11 E12 E13 E14 E15 E16 … EN
QD
E1 E2 E3 E4 E5 E6 E7 E8 E9 E10 E11 E12 E13 E14 E15 E16 … EN
B
Count rate (kCounts/Bq)
QD
HfD
FD
Activity concentration (Bq/mL)
C
FD
100
% FD
0
100
% FD
0
D
HfD
50
% FD
0
50
% FD
0
E
QD
25
% FD
0
25
% FD
0

Fig. 2 Segmentation of the left ventricular wall and the blood pool. Red overlay represents the segmentation of the left ventricle, while the blue area delineates the volume in the ventricle used for the blood and contrast to noise analyses.

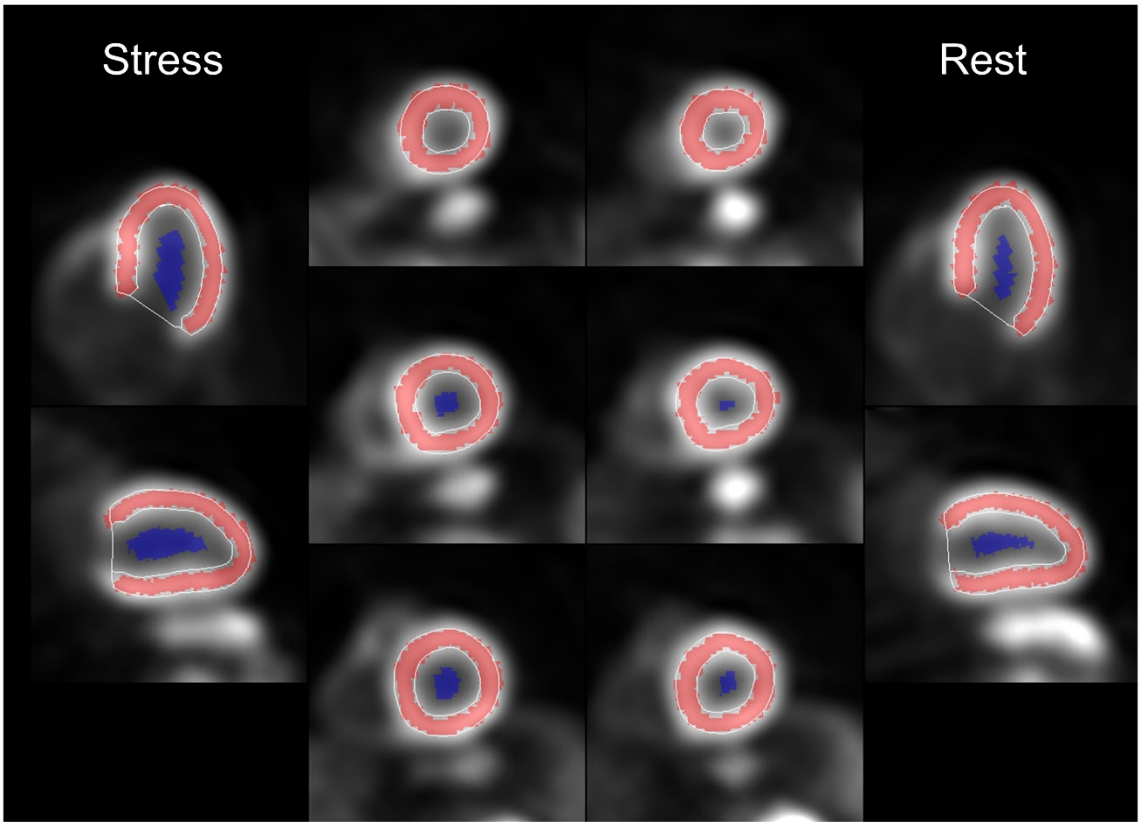

Fig. 3 Diagnostic performance of quantitative perfusion assessment. ROC curves for sTPD (A) and ITPD (B) obtained for the FD, HfD, and QD reconstruction protocols. For sTPD, similar AUC was observed for FD and HfD, while QD was significantly reduced (A).

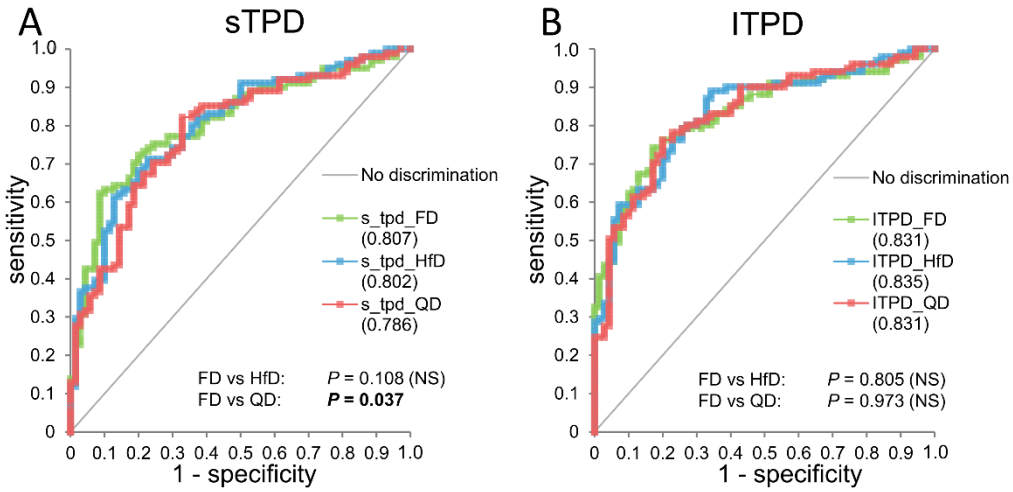

FD = Full dose, HfD = Half-dose, QD = Quarter-dose, ROC = receiver operating characteristic, AUC = Area under ROC curve, sTPD = stress total perfusion deficit, ITPD = ischemic total perfusion deficit, NS= non-significant.

Fig 4. Contrast to noise ratio and noise in the blood pool calculated as the coefficient of variation. Similar contrast to noise ratios was observed for all three reconstruction protocols (Kruskal-Wallis test) (A). Evaluation of the noise in the blood pool, however, showed significantly increased noise for the reconstruction protocols when using HfD and QD data (B). Of note, the figures show the pooled results from the rest and stress scans. Median values are presented above the median line in the box-plots.

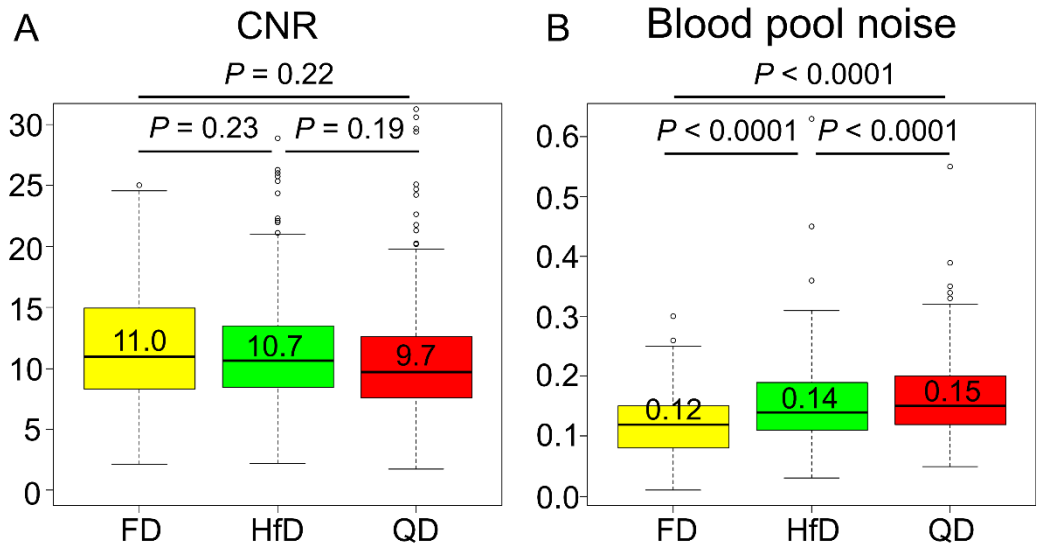

CNR = contrast to noise ratio, FD = Full dose, HfD= half-dose, QD = quarter dose

Fig 5. Case example of stress and rest rubidium MPI with FD, HfD, and QD reconstructions for a 70 years old female. The patient was injected with 1,110MBq ^{82}Rb, with a weight of 79 kg (BMI = 36.5) corresponding to a dose of 14.1 MBq/kg for both the rest and stress MPI scans, respectively. Representative images from short axis, vertical long axis, and extent perfusion polar map are shown for FD (top row), HfD (middle row), and QD (lower row) scans. Similar sTPD and rTPD were reported for all three reconstruction protocols, with increased noise in the blood pool for the dose-reduced reconstructions (CV).

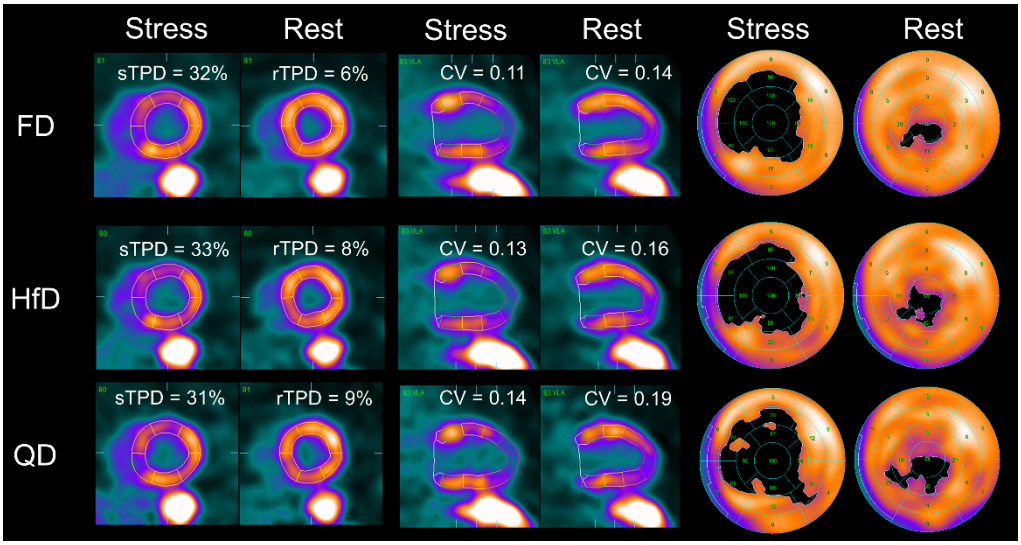

rTPD = rest total perfusion defect, sTPD = stress total perfusion defect, FD = full dose, HfD = half dose and QD = quarter dose, CNR = contrast to noise ratio, BMI = body mass index.

Graphical Abstract

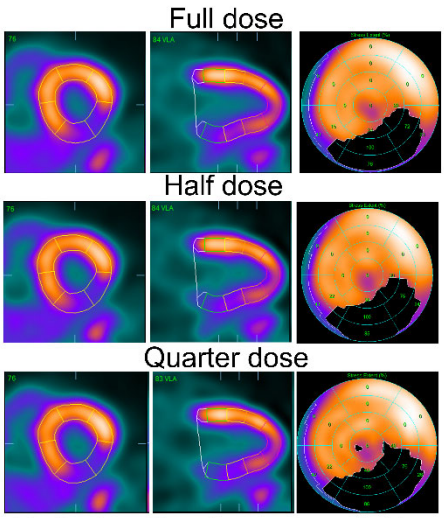

Patient with obstructive right coronary artery stenosis on invasive angiography

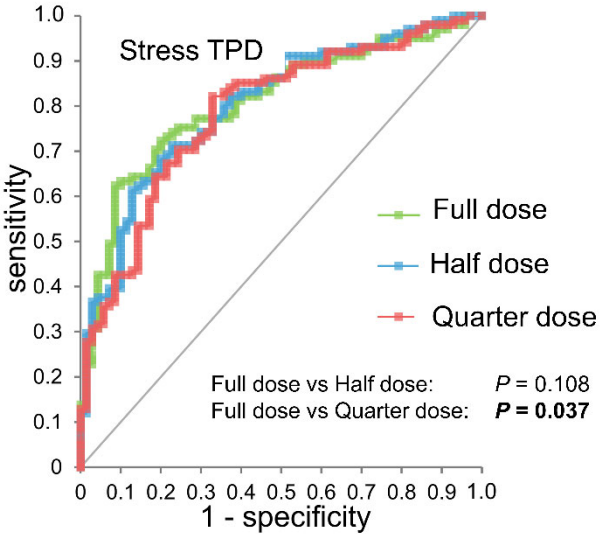

Supplementary Fig. 1 Diagnostic performance of quantitative perfusion assessment for patients with BMI<30 and BMI≥30. ROC curves for sTPD (A,B) and ITPD (C,D) obtained for the FD, HfD, and QD reconstruction protocols. The left column shows the patients with BMI<30 (N=109), while the right shows patients with BMI≥30 (N=62). No significant differences were observed between the FD, HfD and QD assessments for the grouped analyses, similarly no differences in the quantitative assessments were observed between the two groups.

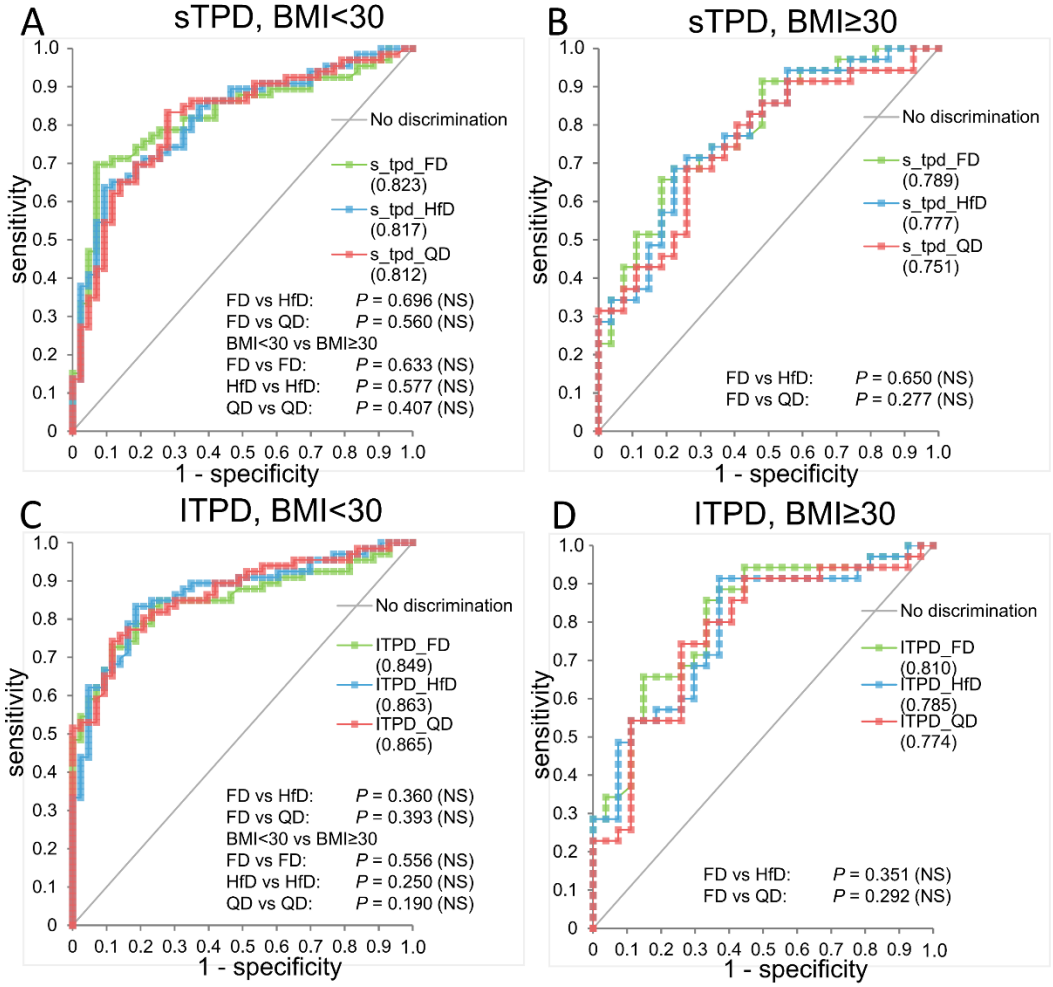

FD = Full dose, HfD = Half-dose, QD = Quarter-dose, ROC = receiver operating characteristic, AUC = Area under ROC curve, sTPD = stress total perfusion deficit, ITPD = ischemic total perfusion deficit, NS= non-significant.

Supplementary Fig. 2 Diagnostic performance of quantitative perfusion assessment. ROC curves for sTPD (A) and ITPD (B) obtained for the FD, HfD, and QD reconstruction protocols. For sTPD, similar AUC was observed for FD and HfD, while QD was significantly reduced (A). Data was reconstructed an OSEM-algorithm using 3 iterations 24 subsets followed by a 8mm Gaussian filtration of the data.

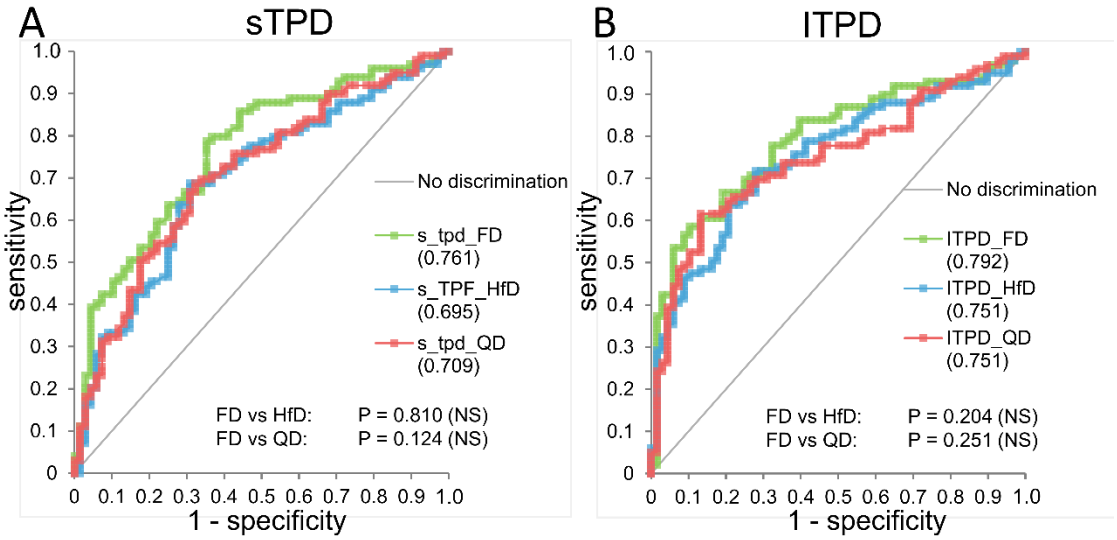

FD = Full dose, HfD = Half-dose, QD = Quarter-dose, ROC = receiver operating characteristic, AUC = Area under ROC curve, sTPD = stress total perfusion deficit, ITPD = ischemic total perfusion deficit, NS= non-significant.

Supplementary Fig 3. Dose-weight corrected Bland-Altman plots of rTPD and sTPD. The Bland-Altman plots were created using the paired data, thus providing bias and confidence intervals for all 171 patients. Increased variability in the rTPD and sTPD are observed for FD/QD as compared to FD/HfD scans. No significant bias was observed for FD/HfD scans (A, C), however, increased bias and a trend to increased variability is observed for FD/QD (B, D). Importantly, no correlation between the dose-weight corrected injection profiles and the bias was observed. The green line indicates the bias, while the yellow lines mark the 95% confidence limits.

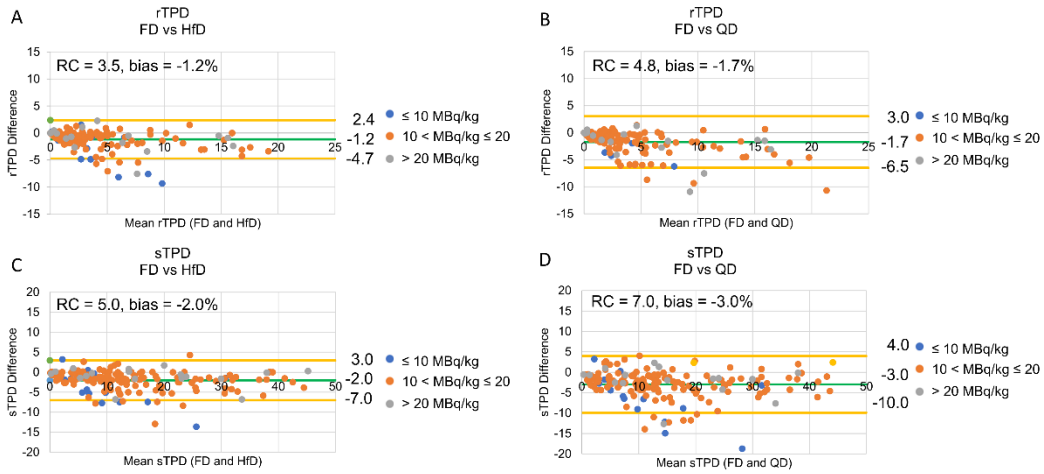

rTPD = rest total perfusion defect, sTPD = stress total perfusion defect, FD = full dose, HfD = half dose and QD = quarter dose. RC = repeatability coefficient

Supplementary Fig. 4 Bland-Altman plots of rTPD and sTPD for patients with BMI<30. The Bland-Altman plots were created using data from the normal-to-overweight patients, thus providing bias and confidence intervals for 109 patients. Increased variability in the rTPD and sTPD are observed for FD/QD as compared to FD/HfD scans. No significant bias was observed for FD and HfD scans (A, C), however, increased bias and a trend to increased variability is observed for FD/QD (B, D). Importantly, no correlation between the dose-weight corrected injection profiles, and the bias was observed. Green line indicates the bias, while the yellow lines mark the 95% confidence limits.

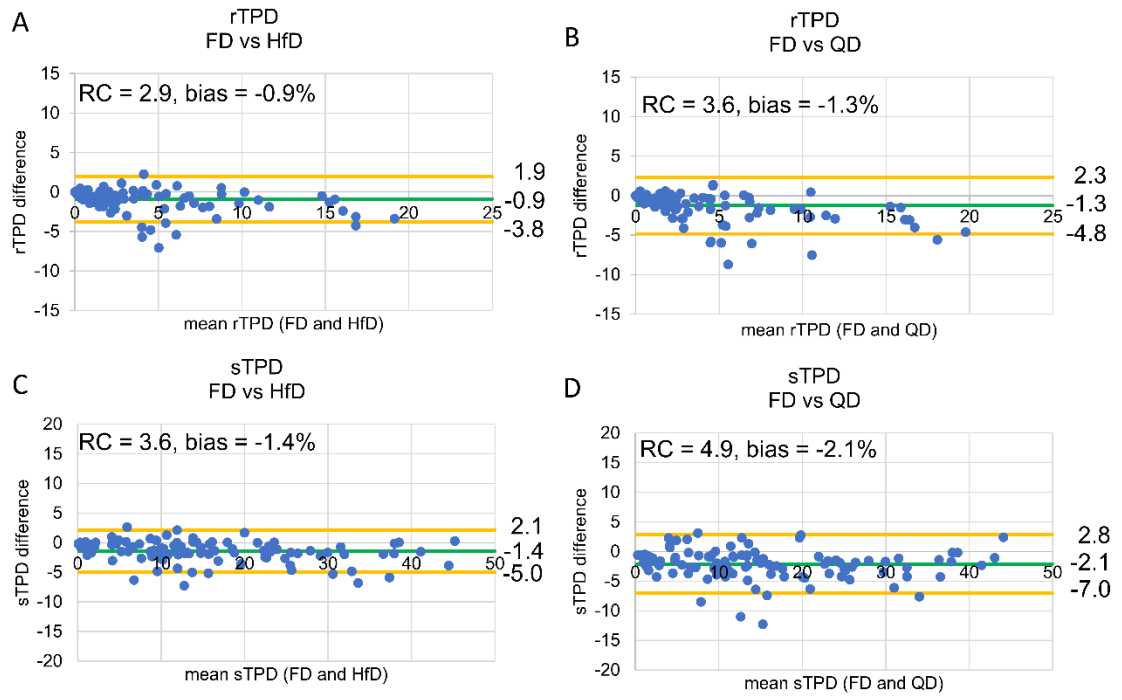

rTPD = rest total perfusion defect, sTPD = stress total perfusion defect, FD = full dose, HfD = half dose and QD = quarter dose. RC = repeatability coefficient

Supplementary Fig. 5 Bland-Altman plots of rTPD and sTPD for patients with BMI≥30. The Bland-Altman plots were created using data from the obese patients, thus providing bias and confidence intervals for 62 patients. Increased variability in the rTPD and sTPD are observed for FD/QD as compared to FD/HfD scans. No significant bias was observed for FD and HfD scans (A, C), however, increased bias and a trend to increased variability is observed for FD/QD (B, D). Importantly, no correlation between the dose-weight corrected injection profiles, and the bias was observed. Green line indicates the bias, while the yellow lines mark the 95% confidence limits.

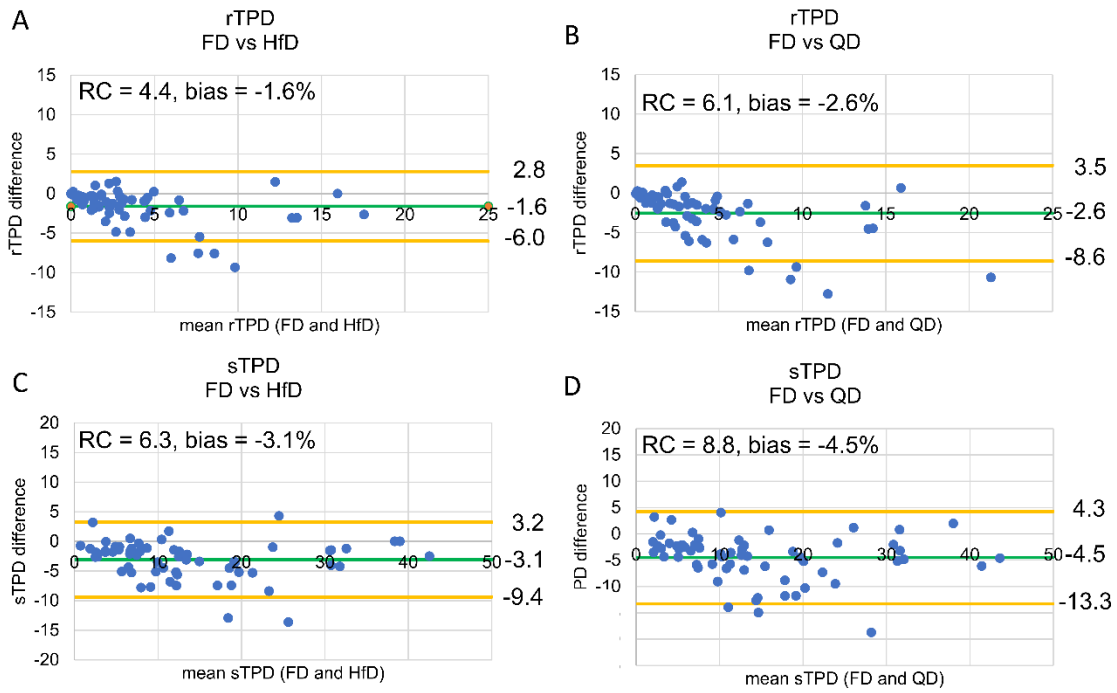

rTPD = rest total perfusion defect, sTPD = stress total perfusion defect, FD = full dose, HfD = half dose and QD = quarter dose. RC = repeatability coefficient

Supplementary Fig 6. Contrast to noise ratio and noise in the blood pool calculated as the coefficient of variation. Similar contrast to noise ratios was observed for the FD and HfD reconstruction protocols, while reduced CNR was observed for the QD reconstructions (Kruskal-Willis test). Evaluation of the noise in the blood pool, however, showed significantly increased noise for the reconstruction protocols when using HfD and QD data. Of note, the figures show the pooled results from the rest and stress scans. Median values are presented above the median line in the box-plots.

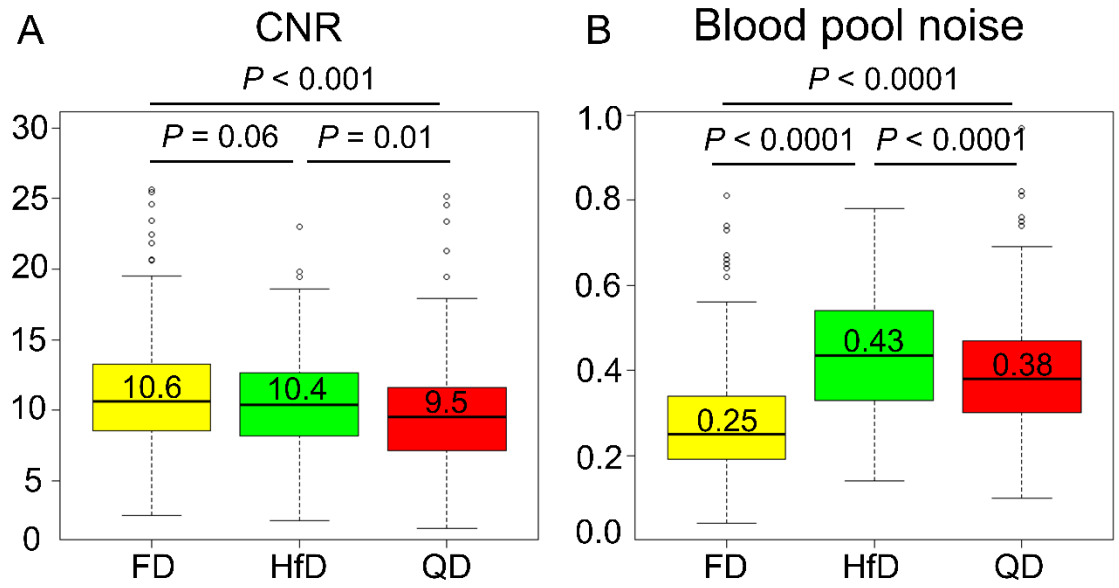

CNR = contrast to noise ratio, FD = Full dose, HfD= half-dose, QD = quarter dose